

# Variable gamma-ray sky at 1 GeV

M.S. Pshirkov<sup>\*1,3</sup> and G.I. Rubtsov <sup>\*\*2</sup>

<sup>1</sup> Universite Libre de Bruxelles, Service de Physique Theorique, CP225, 1050, Brussels, Belgium

<sup>2</sup> Institute for Nuclear Research of the Russian Academy of Sciences, 117312, Moscow, Russia

<sup>3</sup> Pushchino Radio Astronomy Observatory of Lebedev Physical Institute, 142290, Pushchino, Russia

## ABSTRACT

**Aims.** We search for the long-term variability of the  $\gamma$ -ray sky in the energy range  $E > 1$  GeV with 168 weeks of Fermi-LAT data.

**Methods.** We perform a full sky blind search for regions with variable flux looking for deviations from uniformity. We bin the sky into 12288 bins using Healpix package and use Kolmogorov-Smirnov test to compare weekly photon counts in each bin with a constant flux hypothesis. The weekly exposure of Fermi-LAT for each bin is calculated with the Fermi-LAT tools. We consider flux variations in the bin significant if statistical probability of uniformity is less than  $4 \times 10^{-6}$ , which corresponds to 0.05 false detections in the whole set.

**Results.** We identified 117 variable sources, variability of 27 of which has not been reported before. Among the sources with previously unidentified variability there are 25 AGNs belonging to blazar class (11 BL Lacs and 14 FSRQs), one AGN of uncertain type and one pulsar PSR J0633+1746 (Geminga). The observed long term flux variability of Geminga has a statistical significance of  $5.1\sigma$ .

**Key words.** Methods: statistical–BL Lacertae objects: general–quasars: general–Gamma rays: galaxies

## 1. Introduction

Time domain astronomy at different wavelengths from radio to very high-energy gamma-rays is developing very rapidly nowadays. In the high energy (HE) range ( $\geq 100$  MeV) great progress was achieved with advent of the gamma-ray telescope Fermi-LAT (Atwood et al. 2009). Its high sensitivity and almost uniform sky coverage allow one to study variability of large number of sources at these energies on time scales from seconds to years. Sources that demonstrate the most variable behaviour are active galactic nuclei (AGN), primarily of the blazar type (Abdo et al. 2010a). It is well known that these sources exhibit variability on different time scales and at different wavelengths (Carini et al. 1991; Ulrich et al. 1997; Welsh et al. 2011; Rani et al. 2009; Bonning et al. 2009; Soldi et al. 2008; Ghisellini & Tavecchio 2008; Raiteri et al. 2005; Ciprini et al. 2003; Urry et al. 1993). Studies of time variability of these sources are very important for better understanding of AGN engines; they are also essential for assessing the quality of spectral energy distributions obtained from multiwavelength observations made at different epochs.

In this paper we perform a full sky blind search for variable sources. We bin the sky into equal area pixels and search for deviations of photon number counts from the uniformity in time.

## 2. Data and method

The LAT Pass 7 weekly all-sky data publicly available at Fermi mission website<sup>1</sup> were used in this work. The analysis covers the time period of 168 weeks from August 04, 2008 to October 18, 2011, corresponding to mission elapsed time (MET) from 239557417 s to 340622181 s. We use the 'Pass 7 Source' event

class photons with  $E > 1$  GeV and impose an Earth relative zenith angle cut of  $100^\circ$  and rocking angle cut of  $52^\circ$ .

We bin the data week by week using HEALPIX package (Górski et al. 2005) into a map of resolution  $N_{\text{side}} = 32$  in galactic coordinates with 'RING' pixel ordering. Total number of pixels is equal to 12288 and the area of each pixel is 3.6 sq. deg, chosen according to the size of Fermi-LAT point-spread function (PSF) above 1 GeV which is approximately  $1^\circ$ . We estimate integral weekly exposure for each pixel using the standard Fermi-LAT tools *gtlucube* and *gtexpcube* (ScienceTools-v9r23p1-fssc-20110726).

For each pixel we count the number of photons in each of 168 weeks and consider corresponding values of weekly exposure. Typically there are 2–10 photons in a pixel per week except bins with the brightest sources. Cumulative distribution functions (CDFs)  $\mathcal{P}(t)$ ,  $\mathcal{E}(t)$  for both photon counts and exposure are constructed. In the absence of variability, the photon counts would represent a random process with CDF proportional to  $\mathcal{E}(t)$  and thus  $\mathcal{P}(t)$  would follow  $\mathcal{E}(t)$  with deviations caused by a finite number of observed photons. Otherwise  $\mathcal{P}(t)$  would not be statistically compatible with  $\mathcal{E}(t)$ . A Kolmogorov-Smirnov (KS) test is a natural and straightforward way to examine statistical compatibility of the observed photon counts with the distribution given by CDF  $\mathcal{E}(t)$ . The probability that both sets represent the same distribution could be estimated from the maximal value of distance between the functions  $\mathcal{P}(t)$  and  $\mathcal{E}(t)$ . An example CDFs for one of the pixels is shown in Figure 1 and the corresponding flux is shown in Figure 2.

Implemented KS test is most sensitive to the variability at long scales (longer than a week), while transient bursts and flares at shorter time scales may be missed if they are not overwhelmingly strong. On the other hand, our method is sensitive to gradual moderate changes in photon fluxes without any prominent bursts, which could be missed by burst searching techniques.

\* pshirkov@ulb.ac.be

\*\* grisha@ms2.inr.ac.ru

<sup>1</sup> <http://fermi.gsfc.nasa.gov/ssc/data/access/>

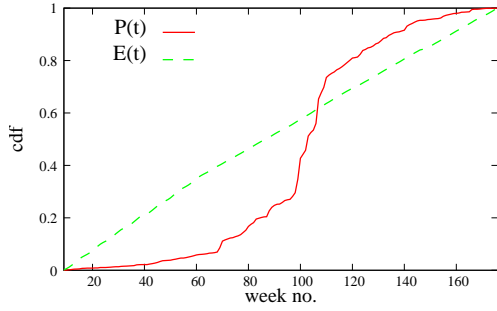


**Fig. 1.** Plot of the cumulative functions  $\mathcal{E}(t)$  and  $\mathcal{P}(t)$  for pixel no.54 ( $l = 261^\circ$ ,  $b = 82.^\circ69$ ). The difference could be easily seen and probability that the photon rate is constant is only  $P = 4 \times 10^{-80}$ .

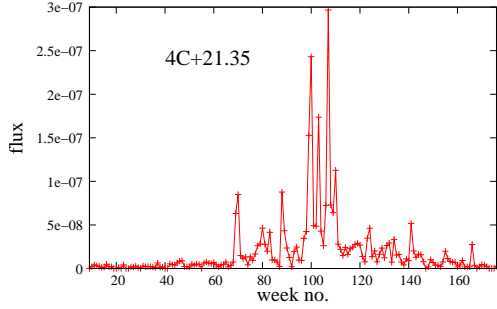


**Fig. 2.** Flux of photons with energies larger than 1 GeV for pixel no.54 (4C+21.35, see Figure 1). The flux is in photons  $\text{cm}^{-2} \text{s}^{-1}$  units.

KS probability is calculated for each pixel – we are interested in pixels with probabilities smaller than the threshold value  $P_0 = 4 \times 10^{-6}$ . This threshold value is set to allow for penalty coming from the large number ( $N_{\text{pix}} = 12288$ ) of trials: the detection criterion is chosen in such a way that the entire search would give a single false detection with the probability of  $P_0 \times N_{\text{pix}} \sim 0.05$ . A map of the probabilities is presented in Figure 4.

### 3. Results

The total number of bins with probabilities smaller than the threshold value  $P_0$  is 151. The source identification for each of these bins is performed as follows. We consider the photons that arrived during several weeks at the epoch of the maximal flux. The center of mass of the spatial distribution of these photons is used as an initial estimate of the source location. We search for sources from 2FGL (The Fermi-LAT Collaboration 2011) catalog in the circle with a radius equal to the error of center of mass estimation which is usually about  $10''$ - $15''$  for  $\sim 20$  photons). For 34 pixels no source is found with the initial estimate: in 31 of them the variability time pattern and photon spatial distribution leads us to identification of the source located in the neighbouring bin and already identified there. In three cases (pixels 2877 and 2749, PMN J1532-1315, and pixel 2299, SBS 0846+513) we have found no counterpart in 2FGL catalog and use Simbad astronomical database. Gamma-ray flares from the latter two sources (PMN J1532-1315 and SBS 0846+513) have been recently reported by Fermi-LAT (Gasparrini & Cutini 2011; Donato & Perkins 2011), but the activity period is outside of the time region of 2FGL catalog. In order to avoid false identifications we performed an additional check in four cases when

two different sources are residing in adjacent pixels: significant difference in the observed luminosity curves confirms that these detections are real. The results are presented in Table 1.

The total number of identified sources is 117; variability of 55 of them was reported in (Abdo et al. 2010a; Tanaka et al. 2011; Schinzel et al. 2011), 35 additional detections were made in numerous Astronomers’s telegrams (ATels, see Appendix) and on the Fermi-LAT blog<sup>2</sup>. That leaves us with 27 sources for which the variability has not been previously detected (see Table 2 and Figures 5–9). We have explicitly checked that flux from these sources is not contaminated with the contribution from the Sun.

For convenience we assign a variability type to the source: a gradual change in the photon flux is referred to as ‘rate’, if the whole variability is dominated by one or several flares we call it ‘flare’ and if these flares are observed by more or less prolonged time span (typically, more than 20 weeks) we designate it as ‘activity’. This morphological distinction is not totally unambiguous: several bright consequent flares could be defined as ‘activity’. On the other hand, gradual changes could take place on a time scales of several tens of weeks, thus fitting the ‘activity’ type as well.

The BL Lacs and the flat-spectrum radio quasars (FSRQs) are represented almost equally in the set of previously unidentified sources: there are 11 BL Lacs, 14 FSRQs, and one AGN of uncertain type (PKS 0644-671). Also there is one pulsar (Geminga) in the list (see Table 2 and Figures 5–9). Both BL Lacs and FSRQs demonstrate two types of variability: gradual change of photon flux (10 out of 25) and flares or increased activity (15 out of 25). Variability of several sources was observed before in other energy ranges: a flare in the near infrared region was observed for B2 1732+38A (ATel #3504 (Carrasco et al. 2011), 1 July 2011), VHE flares of 1ES0806+524 were observed by MAGIC (ATel #3192 (Mariotti 2011), 24 February 2011), and EGRET observed a very bright flare of PKS 2255-282 in December 1997 (Macomb et al. 1999). Pulsed  $\gamma$ -rays from the Geminga pulsar were observed with 1 year of Fermi-LAT data (Abdo et al. 2010c), while the source were considered non-variable. In this paper the long term flux change of Geminga pulsar is detected with KS probability of  $2.3 \times 10^{-7}$ . In present study Geminga is the only pulsar demonstrating variability above our threshold. For comparison the KS probabilities for bins containing Vela, PSR J1709-4429, and Crab pulsars are 25%, 78% and 1.2% respectively. In Crab case it was shown that the observed variability is caused by processes in the Crab nebula rather than the pulsar itself (Buehler et al. 2011). Fermi-LAT collaboration also presented results of observations of three other gamma-ray pulsars (J1836+5925, PSR J2021+4026, and PSR J0007+7303) where no flux variability was observed (Abdo et al. 2010b; Saz Parkinson et al. 2010; Abdo et al. 2012). That makes the case of Geminga even more intriguing.

We note that while 2FGL catalog contains 577 unidentified sources (out of 1873), 153 of which have flux higher than  $2 \times 10^{-9}$  photons  $\text{cm}^{-2} \text{s}^{-1}$ , none of them show variability above our threshold.

It is also worth noting that sources not included in the Table 2 because of being reported either in ATels or on the Fermi blog could have the variability patterns that differ considerably from the reported one. As an example, the flare from the source MG2 J130304+2434 that took place on 3 July 2009 (week no. 56) was reported in ATel #2110 (Hays & Marelli 2009). On the other

<sup>2</sup> <http://fermisky.blogspot.com/>

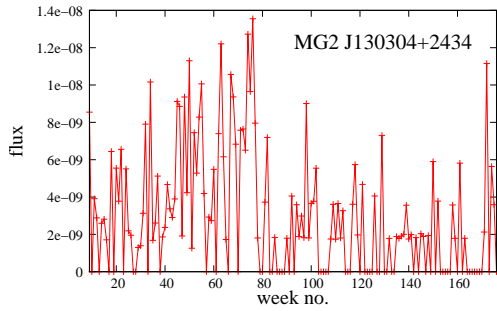


**Fig. 3.** Variability of MG2 J130304+2434. Change of rate could be easily seen.

hand, Figure 3 shows that the flare occurred during the high state of the source, with its flux slowly increasing from the start of the Fermi observations till approximately the 80-th week when it began to decrease.

#### 4. Conclusions

A method for variable sources detection is proposed that uses the KS statistical test. The method is implemented for a full sky blind search for regions with variable flux at energies above 1 GeV using Fermi-LAT 168 weeks data. The search leads to identification of 117 variable sources, the variability of 27 of which has not been reported before. Among the sources with previously unidentified variability there are 25 AGNs belonging to blazar class (11 BL Lacs and 14 FSRQs), one AGN of uncertain type (PKS 0644-671), and one pulsar PSR J0633+1746 (Geminga). The observed long term flux variability of Geminga pulsar has a statistical significance of  $5.1\sigma$ .

#### Appendix

The following ATels are cited in the text: ATel #1933 (Corbel & Reyes 2009), ATel #2048 (Ciprini 2009c), ATel #2049 (Ciprini 2009a), ATel #2104 (Longo et al. 2009), ATel #2110 (Hays & Marelli 2009), ATel #2136 (Ciprini 2009b), ATel #2243 (Tanaka et al. 2009), ATel #2316 (Hays & Escande 2009), ATel #2402 (Sokolovsky et al. 2010), ATel #2413 (Hill & Vandenbroucke 2010), ATel #2539 (Wallace 2010), ATel #2583 (Donato 2010), ATel #2669 (Cutini 2010), ATel #2783 (D'Ammando 2010b), ATel #2829 (Schinzel 2010), ATel #2860 (D'Ammando 2010a), ATel #2907 (Cannon & D'Ammando 2010), ATel #2943 (Ciprini 2010), ATel #3002 (D'Ammando & Vandenbroucke 2010), ATel #3026 (Allafort & D'Ammando 2010), ATel #3171 (Buson & Bastieri 2011), ATel #3192 (Mariotti 2011), ATel #3207 (Allafort 2011), ATel #3452 (Donato & Perkins 2011), ATel #3445 (Gasparrini 2011), ATel #3504 (Carrasco et al. 2011), ATel #3579 (Gasparrini & Cutini 2011), ATel #3670 (Schinzel & Ciprini 2011), ATel #3793 (Ojha et al. 2011).

**Acknowledgements.** We are indebted to P. Tinyakov for numerous helpful discussions at all stages of this work. We thank M. Gustafsson, B. Stern, I. Tkachev and S. Troitsky for useful comments and suggestions. The work was supported in part by the RFBR grants 10-02-01406a, 11-02-01528a, 12-02-91323-SIGa (GR), by the grants of the President of the Russian Federation NS-5525.2010.2 (GR), MK-1632.2011.2 (GR), MK-1582.2010.2 (MP). The work of M.P. is supported in part by the IISN project No. 4.4509.10 and the Belgian Science Policy (IAP VI-11). GR is grateful for the hospitality of ULB Service de Physique Theorique where this study was initiated. The analysis is based on data and software provided by the Fermi Science Support Center (FSSC). The numerical part of the

work is performed at the cluster of the Theoretical Division of INR RAS. This research has made use of NASA's Astrophysics Data System and SIMBAD database, operated at CDS, Strasbourg, France.

#### References

- Abdo, A. A., Ackermann, M., Ajello, M., et al. 2010a, *ApJ*, 722, 520  
 Abdo, A. A., Ackermann, M., Ajello, M., et al. 2010b, *ApJ*, 712, 1209  
 Abdo, A. A., Ackermann, M., Ajello, M., et al. 2010c, *ApJ*, 720, 272  
 Abdo, A. A., Wood, K. S., DeCesar, M. E., et al. 2012, *ApJ*, 744, 146  
 Allafort, A. 2011, *The Astronomer's Telegram*, 3207, 1  
 Allafort, A. & D'Ammando, F. 2010, *The Astronomer's Telegram*, 3026, 1  
 Atwood, W. B., Abdo, A. A., Ackermann, M., et al. 2009, *ApJ*, 697, 1071  
 Bonning, E. W., Bailyn, C., Urry, C. M., et al. 2009, *ApJ*, 697, L81  
 Buehler, R., Scargle, J. D., Blandford, R. D., et al. 2011, *ArXiv e-prints*  
 Buson, S. & Bastieri, D. 2011, *The Astronomer's Telegram*, 3171, 1  
 Cannon, A. & D'Ammando, F. 2010, *The Astronomer's Telegram*, 2907, 1  
 Carini, M. T., Miller, H. R., Noble, J. C., & Sadun, A. C. 1991, *AJ*, 101, 1196  
 Carrasco, L., Carraminana, A., Escobedo, G., et al. 2011, *The Astronomer's Telegram*, 3504, 1  
 Ciprini, S. 2009a, *The Astronomer's Telegram*, 2049, 1  
 Ciprini, S. 2009b, *The Astronomer's Telegram*, 2136, 1  
 Ciprini, S. 2009c, *The Astronomer's Telegram*, 2048, 1  
 Ciprini, S. 2010, *The Astronomer's Telegram*, 2943, 1  
 Ciprini, S., Tosti, G., Raiteri, C. M., et al. 2003, *A&A*, 400, 487  
 Corbel, S. & Reyes, L. C. 2009, *The Astronomer's Telegram*, 1933, 1  
 Cutini, S. 2010, *The Astronomer's Telegram*, 2669, 1  
 D'Ammando, F. 2010a, *The Astronomer's Telegram*, 2860, 1  
 D'Ammando, F. 2010b, *The Astronomer's Telegram*, 2783, 1  
 D'Ammando, F. & Vandenbroucke, J. 2010, *The Astronomer's Telegram*, 3002, 1  
 Donato, D. 2010, *The Astronomer's Telegram*, 2583, 1  
 Donato, D. & Perkins, J. S. 2011, *The Astronomer's Telegram*, 3452, 1  
 Gasparrini, D. 2011, *The Astronomer's Telegram*, 3445, 1  
 Gasparrini, D. & Cutini, S. 2011, *The Astronomer's Telegram*, 3579, 1  
 Ghisellini, G. & Tavecchio, F. 2008, *MNRAS*, 386, L28  
 Górski, K. M., Hivon, E., Banday, A. J., et al. 2005, *ApJ*, 622, 759  
 Hays, E. & Escande, L. 2009, *The Astronomer's Telegram*, 2316, 1  
 Hays, E. & Marelli, M. 2009, *The Astronomer's Telegram*, 2110, 1  
 Hill, A. B. & Vandenbroucke, J. 2010, *The Astronomer's Telegram*, 2413, 1  
 Longo, F., Iafrate, G., Hays, E., & Marelli, M. 2009, *The Astronomer's Telegram*, 2104, 1  
 Macomb, D. J., Gehrels, N., & Shrader, C. R. 1999, *ApJ*, 513, 652  
 Mariotti, M. 2011, *The Astronomer's Telegram*, 3192, 1  
 Ojha, R., Dutka, M., & Torresi, E. 2011, *The Astronomer's Telegram*, 3793, 1  
 Raiteri, C. M., Villata, M., Ibrahimov, M. A., et al. 2005, *A&A*, 438, 39  
 Rani, B., Wiita, P. J., & Gupta, A. C. 2009, *ApJ*, 696, 2170  
 Saz Parkinson, P., Becker, W., Carramiñana, A., et al. 2010, in *Bulletin of the American Astronomical Society*, Vol. 42, AAS/High Energy Astrophysics Division #11, 679  
 Schinzel, F. K. 2010, *The Astronomer's Telegram*, 2829, 1  
 Schinzel, F. K. & Ciprini, S. 2011, *The Astronomer's Telegram*, 3670, 1  
 Schinzel, F. K., Sokolovsky, K. V., D'Ammando, F., et al. 2011, *A&A*, 532, A150  
 Sokolovsky, K. V., Schinzel, F. K., & Wallace, E. 2010, *The Astronomer's Telegram*, 2402, 1  
 Soldi, S., Türlér, M., Paltani, S., et al. 2008, *A&A*, 486, 411  
 Tanaka, Y. T., Stawarz, L., Thompson, D. J., et al. 2011, *ApJ*, 733, 19  
 Tanaka, Y. T., Takahashi, H., & Healey, S. E. 2009, *The Astronomer's Telegram*, 2243, 1  
 The Fermi-LAT Collaboration. 2011, *ArXiv e-prints*  
 Ulrich, M.-H., Maraschi, L., & Urry, C. M. 1997, *ARA&A*, 35, 445  
 Urry, C. M., Maraschi, L., Edelson, R., et al. 1993, *ApJ*, 411, 614  
 Wallace, E. 2010, *The Astronomer's Telegram*, 2539, 1  
 Welsh, B. Y., Wheatley, J. M., & Neil, J. D. 2011, *A&A*, 527, A15

no	Pixel no.	$l^\circ$	$b^\circ$	$N_{\text{phot}}$	$\Phi_{-8}$	$P$	source	2FGL	ref
1	23	345.0	85.6	264	0.29	$2.8 \times 10^{-13}$	MG2 J130304+2434	J1303.1+2435	AT2110
2	44	81.0	82.7	454	0.48	$6.5 \times 10^{-14}$	OP 313	J1310.6+3222	P
3	51	207.0	82.7	467	0.50	$1.4 \times 10^{-6}$	W Comae	J1221.4+2814	P
4	54	261.0	82.7	1700	1.86	$4.3 \times 10^{-80}$	4C+21.35	J1224.9+2122	P2
5	66	97.5	81.2	194	0.20	$3.9 \times 10^{-6}$	5C 12.291	J1308.5+3547	
6	76	247.5	81.2	935	1.02	$2.4 \times 10^{-159}$	4C+21.35	J1224.9+2122	P2
7	77	262.5	81.2	475	0.52	$1.3 \times 10^{-27}$	4C+21.35	J1224.9+2122	P2
8	103	250.7	79.7	216	0.23	$1.4 \times 10^{-6}$	4C +21.35	J1224.9+2122	P2
9	129	196.9	78.3	783	0.84	$7.7 \times 10^{-40}$	Ton 599	J1159.5+2914	P
10	335	162.7	70.9	468	0.48	$1.9 \times 10^{-16}$	S4 1144+40	J1146.9+4000	B165
11	373	61.1	69.4	188	0.20	$1.8 \times 10^{-9}$	J1424+3615	J1424+3615	
12	378	93.2	69.4	332	0.33	$4.2 \times 10^{-10}$	B3 1343+451	J1345.4+4453	AT3793
13	381	112.5	69.4	433	0.43	$1.9 \times 10^{-11}$	GB 1310+487	J1312.8+4828	AT2316
14	438	111.0	67.9	343	0.33	$2.1 \times 10^{-22}$	GB 1310+487	J1312.8+4828	AT2316
15	532	295.3	66.4	461	0.54	$7.3 \times 10^{-9}$	MG1 J123931+0443	J1239.5+0443	AT3445
16	564	108.5	64.9	201	0.19	$1.4 \times 10^{-7}$	CLASS J1333+5057	J1333.5+5058	
17	571	145.6	64.9	370	0.36	$7.5 \times 10^{-61}$	OM 484	J1153.2+4935	B153
18	598	288.5	64.9	855	1.00	$3.3 \times 10^{-56}$	3C 273	J1229.1+0202	P
19	670	292.5	63.4	301	0.35	$2.1 \times 10^{-6}$	3C 273	J1229.1+0202	P
20	998	304.8	57.4	1925	2.26	$5.1 \times 10^{-57}$	3C 279	J1256.1-0547	P
21	1014	9.8	55.9	967	1.10	$6.3 \times 10^{-123}$	PKS 1502+106	J1504.3+1029	P
22	1106	9.4	54.3	598	0.68	$2.0 \times 10^{-62}$	PKS 1502+106	J1504.3+1029	P
23	1107	13.1	54.3	1414	1.60	$4.1 \times 10^{-212}$	PKS 1502+106	J1504.3+1029	P
24	1159	208.1	54.3	443	0.48	$3.4 \times 10^{-11}$	MG2 J101241+2439	J1012.6+2440	P
25	1203	12.6	52.8	358	0.41	$4.1 \times 10^{-24}$	PKS 1502+106	J1504.3+1029	P
26	1448	148.3	49.7	744	0.64	$3.5 \times 10^{-60}$	S4 1030+61	J1033.9+6050	P
27	1483	265.0	49.7	321	0.38	$2.0 \times 10^{-10}$	PKS 1118-05	J1121.5-0554	B71
28	1499	318.3	49.7	310	0.36	$8.1 \times 10^{-7}$	PMN J1332-1256	J1332.5-1255	
29	1585	236.2	48.1	267	0.31	$3.0 \times 10^{-12}$	PMN J1016+0512	J1016.0+0513	P
30	1631	23.3	46.6	374	0.42	$7.6 \times 10^{-10}$	PKS 1551+130	J1553.5+1255	P
31	1654	94.7	46.6	465	0.40	$1.4 \times 10^{-9}$	GB6 J1542+6129	J1542.9+6129	P
32	1700	237.4	46.6	283	0.33	$3.3 \times 10^{-12}$	PMN J1016+0512	J1016.0+0513	P
33	1798	175.5	45.0	729	0.73	$1.2 \times 10^{-44}$	S4 0917+44	J0920.9+4441	P
34	1970	320.8	43.4	538	0.62	$8.3 \times 10^{-15}$	PMN J1344-1723	J1344.2-1723	
35	2005	60.5	41.8	1193	1.23	$2.7 \times 10^{-22}$	4C+38.41	J1635.2+3810	P
36	2006	63.3	41.8	808	0.82	$1.7 \times 10^{-6}$	NRAO 512	J1640.7+3945	P3
37	2237	351.6	40.2	2977	3.47	$1.5 \times 10^{-61}$	PKS 1510-08	J1512.8-0906	P
38	2299	167.3	38.7	276	0.26	$8.1 \times 10^{-13}$	SBS 0846+513		AT3452
39	2338	277.0	38.7	527	0.60	$2.4 \times 10^{-33}$	PKS 1124-186	J1126.6-1856	AT3207
40	2392	67.5	37.2	254	0.25	$1.1 \times 10^{-7}$	B3 1708+433	J1709.7+4319	AT3026
41	2475	300.9	37.2	940	1.06	$1.4 \times 10^{-11}$	PKS 1244-255	J1246.7-2546	P
42	2520	68.9	35.7	498	0.50	$1.9 \times 10^{-26}$	B3 1708+433	J1709.7+4319	AT3026
43	2569	206.7	35.7	551	0.60	$8.9 \times 10^{-12}$	OJ 287	J0854.8+2005	P
44	2683	165.9	34.2	258	0.24	$4.7 \times 10^{-7}$	1ES 0806+524	J0809.8+5218	VHE AT3192
45	2749	351.6	34.2	628	0.73	$1.4 \times 10^{-77}$	PMN J1532-1319		AT3579
46	2810	164.5	32.8	254	0.24	$1.9 \times 10^{-7}$	1ES 0806+524	J0809.8+5218	VHE AT3192
47	2811	167.3	32.8	537	0.51	$9.6 \times 10^{-16}$	1ES 0806+524	J0809.8+5218	VHE AT3192
48	2815	178.6	32.8	735	0.74	$1.2 \times 10^{-6}$	S4 0814+42	J0818.2+4223	P
49	2844	260.2	32.8	290	0.33	$1.3 \times 10^{-7}$	1RXS J102658.5-174905	J1026.7-1749	
50	2877	353.0	32.8	431	0.50	$3.9 \times 10^{-15}$	PMN J1532-1319		AT3579
51	2903	64.7	31.4	404	0.41	$2.1 \times 10^{-16}$	B2 1732+38A	J1734.3+3858	IR AT3504
52	2916	101.2	31.4	466	0.38	$9.2 \times 10^{-21}$	S4 1749+70	J1748.8+7006	AT3171
53	3043	99.8	30.0	830	0.67	$4.0 \times 10^{-8}$	S4 1749+70	J1748.8+7006	AT3171
54	3150	39.4	28.6	371	0.40	$1.9 \times 10^{-21}$	PKS 1717+177	J1719.3+1744	P

no	Pixel no.	$l^\circ$	$b^\circ$	$N_{\text{phot}}$	$\Phi_{-8}$	$P$	source	2FGL	ref
55	3187	143.4	28.6	1845	1.49	$4.0 \times 10^{-10}$	S5 0716+71	J0721.9+7120	P
56	3194	163.1	28.6	756	0.69	$1.7 \times 10^{-50}$	GB6 J0742+5444	J0742.6+5442	AT3445
57	3246	309.4	28.6	451	0.50	$2.7 \times 10^{-10}$	PKS 1313-333	J1315.9-3339	B122
58	3489	272.8	25.9	247	0.28	$1.3 \times 10^{-7}$	PKS B1043-291	J1045.5-2931	
59	3540	57.7	24.6	557	0.58	$1.1 \times 10^{-16}$	RX J1754.1+3212	J1754.3+3212	
60	3554	97.0	24.6	896	0.73	$1.1 \times 10^{-50}$	S4 1849+67	J1849.4+6706	P
61	3598	220.8	24.6	439	0.50	$1.4 \times 10^{-7}$	PKS 0829+046	J0831.9+0429	
62	3963	165.9	20.7	462	0.44	$5.9 \times 10^{-9}$	GB6 J0654+5042	J0654.5+5043	P
63	4000	270.0	20.7	325	0.36	$1.7 \times 10^{-15}$	PKS 1021-323	J1023.8-3248	
64	4021	321.1	20.7	813	0.90	$1.8 \times 10^{-44}$	PKS 1454-354	J1457.4-3540	P
65	4092	170.2	19.5	457	0.45	$5.9 \times 10^{-10}$	B3 0650+453	J0654.2+4514	P
66	4097	184.2	19.5	613	0.64	$9.7 \times 10^{-8}$	B2 0716+33	J0719.3+3306	P
67	4110	220.8	19.5	324	0.37	$2.0 \times 10^{-8}$	OJ 014	J0811.4+0149	
68	4116	237.7	19.5	412	0.48	$5.7 \times 10^{-8}$	BZQ J0850-1213	J0850.2-1212	B102,114
69	4149	330.5	19.5	463	0.51	$2.6 \times 10^{-7}$	PKS 1454-354	J1457.4-3540	P
70	4402	322.0	17.0	1495	1.63	$7.8 \times 10^{-36}$	PKS B1424-418	J1428.0-4206	AT2104,2583
71	4541	351.6	15.7	1505	1.69	$1.5 \times 10^{-19}$	PKS 1622-253	J1625.7-2526	P
72	4614	198.3	14.5	338	0.37	$1.2 \times 10^{-6}$	MG2 J071354+1934	J0714.0+1933	P
73	4616	203.9	14.5	799	0.88	$4.0 \times 10^{-19}$	4C+14.23	J0725.3+1426	AT2243
74	4625	229.2	14.5	402	0.46	$1.1 \times 10^{-6}$	PKS 0805-07	J0808.2-0750	AT2048,2136
75	4742	196.9	13.2	413	0.44	$5.7 \times 10^{-17}$	MG2 J071354+1934	J0714.0+1933	P
76	4744	202.5	13.2	353	0.38	$1.9 \times 10^{-6}$	4C+14.23	J0725.3+1426	AT2243
77	4753	227.8	13.2	707	0.82	$5.5 \times 10^{-16}$	PKS 0805-07	J0808.2-0750	AT2048,2136
78	4881	229.2	12.0	556	0.64	$3.4 \times 10^{-14}$	PKS 0805-07	J0808.2-0750	AT2048,2136
79	4932	11.2	10.8	1337	1.54	$2.7 \times 10^{-16}$	PKS 1730-13	J1733.1-1307	AT3002
80	5119	178.6	9.6	619	0.64	$9.9 \times 10^{-8}$	B2 0619+33	J0622.9+3326	AT2829
81	5165	308.0	9.6	1011	1.06	$2.6 \times 10^{-7}$	PMN J1326-5256	J1326.7-5254	
82	5637	195.5	4.8	52455	56.6	$2.3 \times 10^{-7}$	PSR J0633+1746	J0633.9+1746	
83	5248	180.0	8.4	1212	1.26	$1.1 \times 10^{-46}$	B2 0619+33	J0622.9+3326	AT2829
84	5777	227.8	3.6	2002	2.3	$3.2 \times 10^{-12}$	PKS 0727-11	J0730.2-1141	AT2860
85	6596	12.7	-4.8	1854	2.1	$4.6 \times 10^{-7}$	PKS 1830-211	J1833.6-2104	AT2943
86	6608	46.4	-4.8	1198	1.3	$3.6 \times 10^{-7}$	RX J1931.1+0937	J1931.1+0938	
87	6711	336.1	-4.8	1717	1.8	$2.6 \times 10^{-9}$	PMN J1650-5044	J1650.1-5044	
88	6724	11.2	-6.0	1945	2.2	$2.9 \times 10^{-15}$	PKS 1830-211	J1833.6-2104	AT2943
89	7101	351.6	-8.4	1553	1.71	$5.4 \times 10^{-38}$	PMN J1802-3940	J1802.6-3940	
90	7155	144.8	-9.6	696	0.67	$3.4 \times 10^{-7}$	4C+47.08	J0303.5+4713	
91	7265	92.8	-10.8	1664	1.65	$1.9 \times 10^{-46}$	BL Lac	J2202.8+4216	P
92	7413	150.5	-12.0	931	0.93	$1.2 \times 10^{-8}$	NGC 1275	J0319.8+4130	P
93	7494	16.9	-13.2	868	0.98	$1.2 \times 10^{-7}$	PKS B1908-201	J1911.1-2005	P
94	7542	151.9	-13.2	1202	1.21	$6.7 \times 10^{-9}$	NGC 1275	J0319.8+4130	P
95	7569	227.8	-13.2	539	0.61	$2.3 \times 10^{-8}$	PKS 0627-199	J0629.3-2001	B174
96	7662	130.8	-14.5	868	0.84	$9.1 \times 10^{-23}$	OC 457	J0136.9+4751	P
97	7750	16.9	-15.7	801	0.91	$7.5 \times 10^{-36}$	TXS 1920-211	J1923.5-2105	P
98	7921	139.2	-17.0	2228	2.2	$3.6 \times 10^{-10}$	3C 66A	J0222.6+4302	P
99	7993	341.7	-17.0	512	0.54	$3.5 \times 10^{-6}$	PKS 1821-525	J1825.1-5231	
100	8030	84.4	-18.2	677	0.70	$5.8 \times 10^{-17}$	B2 2155+31	J2157.4+3129	P
101	8197	195.5	-19.5	896	1.01	$4.9 \times 10^{-20}$	TXS 0506+056	J0509.4+0542	
102	8525	36.6	-23.3	431	0.50	$8.0 \times 10^{-16}$	PKS 2023-07	J2025.6-0736	P
103	8653	38.0	-24.6	563	0.65	$1.3 \times 10^{-31}$	PKS 2023-07	J2025.6-0736	P
104	8675	99.8	-24.6	658	0.68	$4.8 \times 10^{-23}$	B2 2308+34	J2311.0+3425	AT2783
105	8867	278.4	-25.9	508	0.50	$1.1 \times 10^{-13}$	PKS 0644-671	J0644.2-6713	
106	9074	140.6	-28.6	428	0.44	$1.4 \times 10^{-17}$	B2 0200+30	J0204.0+3045	B134
107	9077	149.1	-28.6	821	0.86	$1.2 \times 10^{-31}$	4C+28.07	J0237.8+2846	AT3670
108	9094	196.9	-28.6	466	0.53	$1.6 \times 10^{-22}$	PKS 0440-00	J0442.7-0017	AT2049

no	Pixel no.	$l^\circ$	$b^\circ$	$N_{\text{phot}}$	$\Phi_{-8}$	$P$	source	2FGL	ref
109	9197	128.0	-30.0	512	0.53	$1.1 \times 10^{-17}$	4C 31.03	J0112.8+3208	
110	9369	250.3	-31.4	3416	3.67	$1.6 \times 10^{-90}$	PKS 0537-441	J0538.8-4405	P
111	9431	66.1	-32.8	395	0.44	$1.1 \times 10^{-8}$	PKS 2144+092	J2147.3+093	P
112	9477	195.5	-32.8	588	0.67	$1.9 \times 10^{-15}$	PKS 0420-01	J0423.2-0120	AT2402
113	9498	254.5	-32.8	946	1.01	$7.7 \times 10^{-101}$	PMN J0531-4827	J0532.0-4826	AT2907
114	9615	222.2	-34.2	259	0.30	$3.6 \times 10^{-8}$	PKS 0454-234	J0457.0-2325	P
115	9616	225.0	-34.2	341	0.38	$7.5 \times 10^{-14}$	PKS 0454-234	J0457.0-2325	P
116	9743	223.6	-35.7	1282	1.43	$5.8 \times 10^{-118}$	PKS 0454-234	J0457.0-2325	P
117	9776	316.4	-35.7	483	0.50	$2.4 \times 10^{-17}$	PKS 2142-75	J2147.4-7534	AT2539
118	9822	84.4	-37.2	782	0.85	$5.2 \times 10^{-23}$	3C 454.3	J2253.9+1609	P
119	9823	87.2	-37.2	1832	1.98	$1.5 \times 10^{-72}$	3C 454.3	J2253.9+1609	P
120	9904	315.0	-37.2	530	0.55	$1.8 \times 10^{-15}$	PKS 2142-75	J2147.4-7534	AT2539
121	9947	77.3	-38.7	500	0.55	$4.2 \times 10^{-13}$	CTA 102	J2232.4+1143	P
122	9951	88.6	-38.7	417	0.45	$1.8 \times 10^{-6}$	3C 454.3	J2253.9+1609	P
123	9950	85.8	-38.7	10048	11.0	$7.4 \times 10^{-539}$	3C 454.3	J2253.9+1609	P
124	9975	156.1	-38.7	1097	1.19	$7.5 \times 10^{-247}$	AO 0235+164	J0238.7+1637	P
125	10094	129.4	-40.2	838	0.89	$4.4 \times 10^{-8}$	S2 0109+22	J0112.1+2245	P
126	10104	157.5	-40.2	522	0.57	$4.0 \times 10^{-37}$	AO 0235+164	J0238.7+1637	P
127	10108	168.8	-40.2	564	0.62	$1.8 \times 10^{-12}$	PKS 0306+102	J0309.1+1027	
128	10173	351.6	-40.2	648	0.70	$8.4 \times 10^{-11}$	PKS 2052-47	J2056.2-4715	P
129	10368	187.3	-43.4	339	0.39	$4.1 \times 10^{-15}$	PKS 0336-01	J0339.4-0144	
130	10386	239.5	-43.4	1411	1.54	$1.8 \times 10^{-50}$	PKS 0426-380	J0428.6-3756	P
131	10387	242.4	-43.4	440	0.48	$8.9 \times 10^{-7}$	PKS 0426-380	J0428.6-3756	P
132	10508	241.5	-45.0	683	0.75	$1.3 \times 10^{-6}$	PKS 0426-380	J0428.6-3756	P
133	10692	91.6	-48.1	289	0.32	$4.8 \times 10^{-9}$	PKS 2325+093	J2327.5+0940	P
134	10711	152.7	-48.1	569	0.63	$6.2 \times 10^{-22}$	MG1 J021114+1051	J0211.2+1050	P
135	10775	358.4	-48.1	582	0.64	$1.1 \times 10^{-12}$	MH 2136-428	J2139.3-4236	P
136	10779	11.7	-49.7	263	0.29	$1.2 \times 10^{-7}$	PMN J2145-3357	J2144.8-3356	
137	10840	215.0	-49.7	186	0.21	$1.1 \times 10^{-7}$	PKS 0347-211	J0350.0-2104	P
138	10847	238.3	-49.7	337	0.37	$3.5 \times 10^{-6}$	PKS 0402-362	J0403.9-3604	AT2413
139	10889	19.0	-51.3	1101	1.24	$6.0 \times 10^{-8}$	PKS 2155-304	J2158.8-3013	P
140	10965	282.1	-51.3	294	0.29	$2.9 \times 10^{-7}$	PKS 0235-618	J0237.1-6136	AT2669
141	10992	16.2	-52.8	1217	1.36	$2.2 \times 10^{-7}$	PKS 2155-304	J2158.8-3013	P
142	11131	163.1	-54.3	454	0.52	$7.3 \times 10^{-17}$	PKS 0215+015	J0217.9+0143	P
143	11495	213.7	-60.4	572	0.64	$5.2 \times 10^{-11}$	PKS 0301-243	J0303.4-2407	P
144	11506	263.2	-60.4	470	0.51	$9.1 \times 10^{-8}$	PKS 0244-470	J0245.9-4652	P
145	11572	210.8	-61.9	563	0.63	$1.9 \times 10^{-9}$	PKS 0250-225	J0252.7-2218	AT1933
146	11586	277.1	-61.9	625	0.67	$3.5 \times 10^{-13}$	PKS 0208-512	J0210.7-5102	P
147	11597	329.2	-61.9	267	0.28	$3.2 \times 10^{-11}$	PKS 2326-502	J2329.2-4956	AT2783
148	11598	333.9	-61.9	508	0.55	$1.5 \times 10^{-27}$	PKS 2326-502	J2329.2-4956	AT2783
149	11670	332.5	-63.5	805	0.87	$9.0 \times 10^{-62}$	PKS 2326-502	J2329.2-4956	AT2783
150	11680	23.8	-64.9	387	0.43	$2.1 \times 10^{-7}$	PKS 2255-282	J2258.0-2759	
151	11933	65.8	-70.9	953	1.09	$1.4 \times 10^{-90}$	PMN J2345-1555	J2345.0-1553	P

**Table 1.** List of pixels demonstrating variability exceeding threshold value ( $P < 4 \times 10^{-6}$ ).  $l, b$  are the galactic coordinates of the center of the pixel,  $N_{\text{phot}}$  is the total number of photons observed in the pixel,  $\Phi_{-8}$  is the average flux from the pixel  $\Phi_{-8} \equiv \Phi/10^{-8}$  photons  $\text{cm}^{-2} \text{s}^{-1}$ : the total number of photons divided by the total exposure,  $P$  is the KS probability, the designations of the identified source in the literature and in the 2FGL catalog are in the 8th and 9th columns. Previous references to the variability of the source are presented in the last column: P stands for paper (Abdo et al. 2010a), P2 for (Tanaka et al. 2011), P3 for (Schinzel et al. 2011), ATNNNN for ATel #NNNN, and BNNN indicates that the outburst from the source was mentioned on the Fermi blog in the NNNth weekly report. ATNNNN with prefix VHE or IR indicate that flare was observed (and reported in corresponding ATel) in some other energy range: very high energy (larger than 100 GeV) or in the infrared. All the references for the ATels are listed in the Appendix.



no	Pixel no.	$l^\circ$	$b^\circ$	$N_{\text{phot}}$	$\Phi_{-8}$	$P$	source	source type	variability	weeks
1	66	97.5	81.2	194	0.20	$3.9 \times 10^{-6}$	5C 12.291	Q	A	30–60
2	373	61.1	69.4	188	0.20	$1.8 \times 10^{-9}$	J1424+3615	B	A	140–160
3	564	108.5	64.9	201	0.19	$1.4 \times 10^{-7}$	CLASS J1333+5057	Q	R	-
4	1499	318.3	49.7	310	0.36	$8.1 \times 10^{-7}$	PMN J1332-1256	Q	R	-
5	1970	320.8	43.4	538	0.62	$8.3 \times 10^{-15}$	PMN J1344-1723	Q	R	-
6	2811	167.3	32.8	537	0.51	$9.6 \times 10^{-16}$	1ES 0806+524	B	R	-
7	2844	260.2	32.8	290	0.33	$1.3 \times 10^{-7}$	1RXS J102658.5-174905	B	R,F	176
8	2903	64.7	31.4	404	0.41	$2.1 \times 10^{-16}$	B2 1732+38A	B	F	40–50
9	3489	272.8	25.9	247	0.28	$1.3 \times 10^{-7}$	PKS B1043-291	Q	A	100–120
10	3540	57.7	24.6	557	0.58	$1.1 \times 10^{-16}$	RX J1754.1+3212	B	F	149–153
11	3598	220.8	24.6	439	0.50	$1.4 \times 10^{-7}$	PKS 0829+046	B	F	73
12	4000	270.0	20.7	325	0.36	$1.7 \times 10^{-15}$	PKS 1021-323	Q	R	-
13	4110	220.8	19.5	324	0.37	$2.0 \times 10^{-8}$	OJ 014	B	R	-
14	5165	308.0	9.6	1011	1.06	$2.6 \times 10^{-7}$	PMN J1326-5256	B	F	9,32
15	5637	195.5	4.8	52455	56.6	$2.3 \times 10^{-7}$	PSR J0633+1746	PSR	R	-
16	6608	46.4	-4.8	1198	1.3	$3.6 \times 10^{-7}$	RX J1931.1+0937	B	R	-
17	6711	336.1	-4.8	1717	1.8	$2.6 \times 10^{-9}$	PMN J1650-5044	Q	R	-
18	7101	351.6	-8.4	1553	1.71	$5.4 \times 10^{-38}$	PMN J1802-3940	Q	A	60-100
19	7155	144.8	-9.6	696	0.67	$3.4 \times 10^{-7}$	4C+47.08	B	A	100-140
20	7993	341.7	-17.0	512	0.54	$3.5 \times 10^{-6}$	PKS 1821-525	Q	R	-
21	8197	195.5	-19.5	896	1.01	$4.9 \times 10^{-20}$	TXS 0506+056	B	A	137-140, 169-172
22	8867	278.4	-25.9	508	0.50	$1.1 \times 10^{-13}$	PKS 0644-671	AGN	R	-
23	9197	128.0	-30.0	512	0.53	$1.1 \times 10^{-17}$	4C 31.03	Q	A	30-50,148
24	10108	168.8	-40.2	564	0.62	$1.8 \times 10^{-12}$	PKS 0306+102	Q	F	141-147
25	10368	187.3	-43.4	339	0.39	$4.1 \times 10^{-15}$	PKS 0336-01	Q	F	131
26	10779	11.7	-49.7	263	0.29	$1.2 \times 10^{-7}$	PMN J2145-3357	Q	A	74,91,121
27	11680	23.8	-64.9	387	0.43	$2.1 \times 10^{-7}$	PKS 2255-282	Q	A	60–80, 136

**Table 2.** List of sources with previously unreported variability. Additional columns describe source type: BL Lac (B), FSRQ (Q), AGN of uncertain type (AGN), or pulsar (PSR), variability type: gradual increase or decrease in photon flux rate (R), flares (F) or longer period of increased activity (A); in case of flares or activity the temporal localization of events is given in the last column.

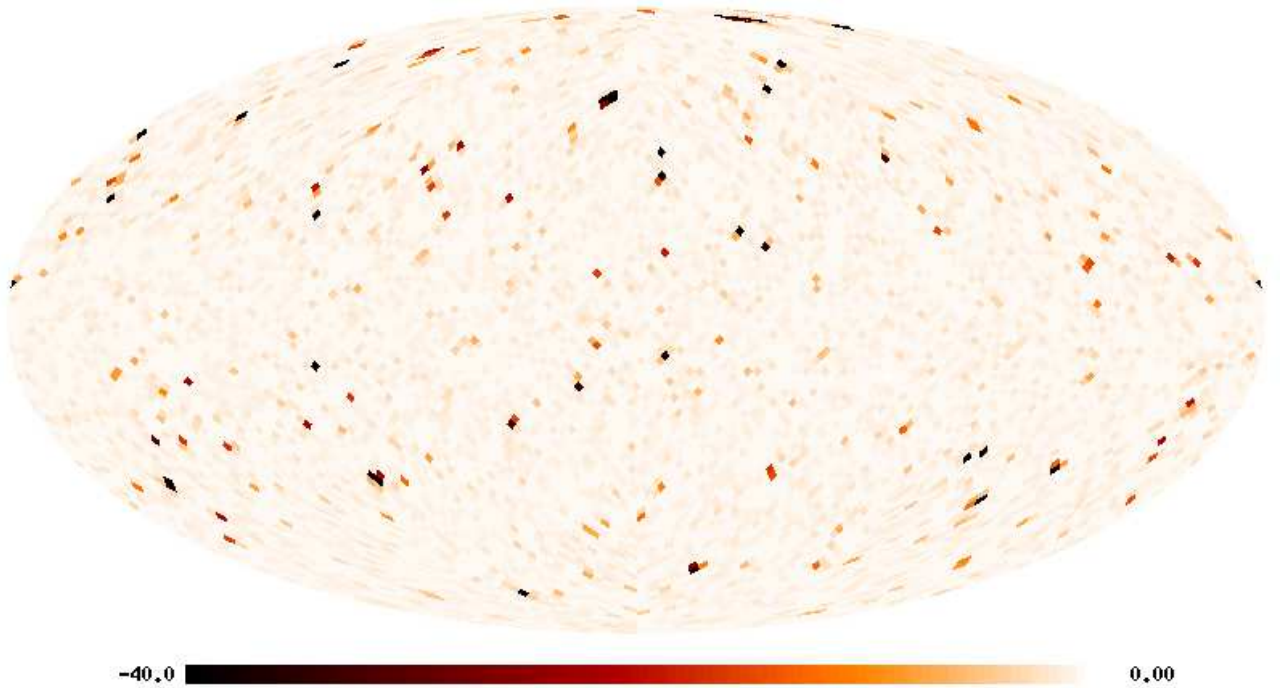


**Fig. 4.** Map of Fermi-LAT variability at 1 GeV in galactic coordinates. Pixel color represents base 10 logarithm of Kolmogorov-Smirnov probability of the uniformity of the observed flux. The galactic center is in the center of the figure,  $l = 180^\circ$  is on the left.

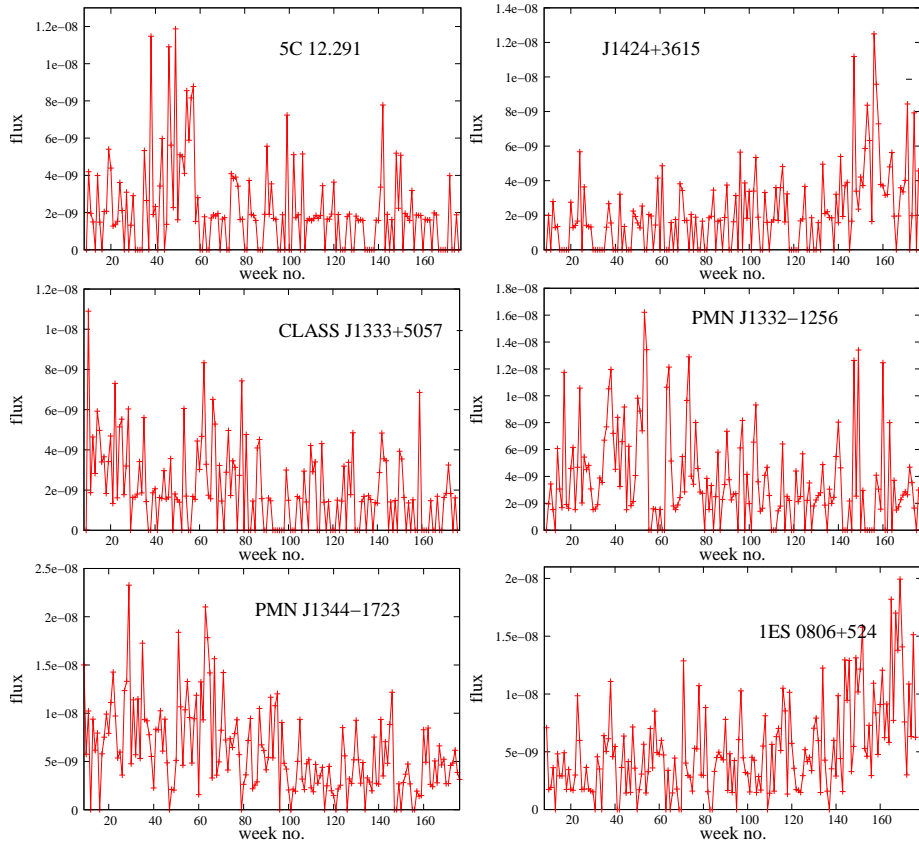


**Fig. 5.** Luminosity curves for variable sources listed in the Table 2. The flux is in photons  $\text{cm}^{-2} \text{s}^{-1}$  units.

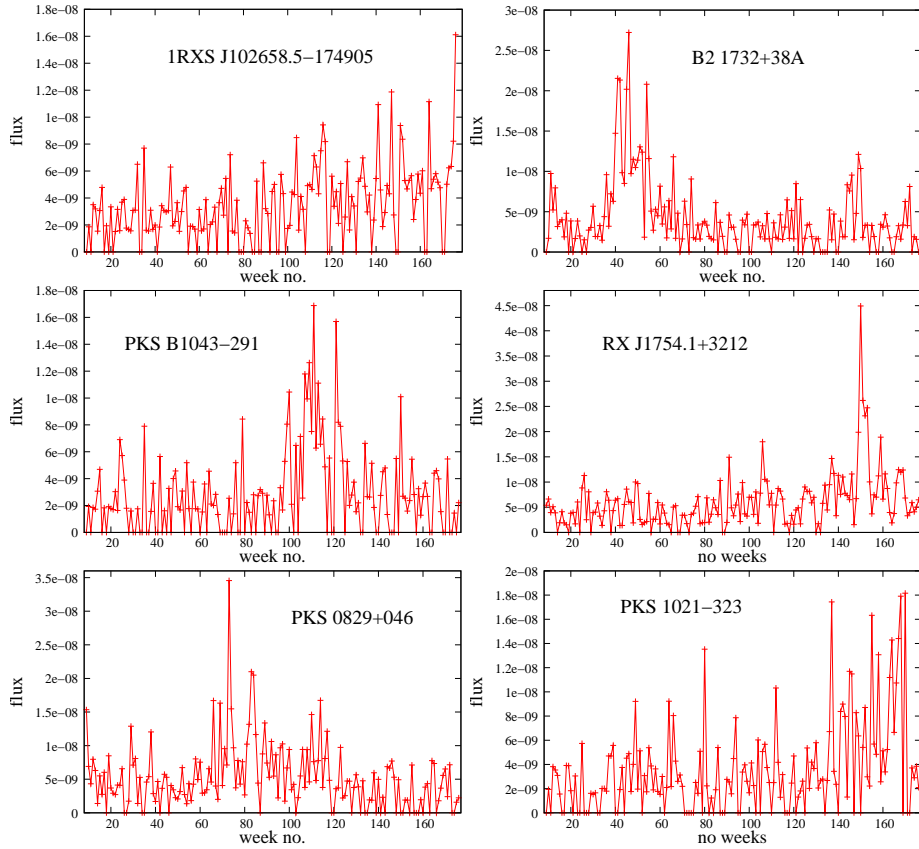


**Fig. 6.** The same as in Figure 5.



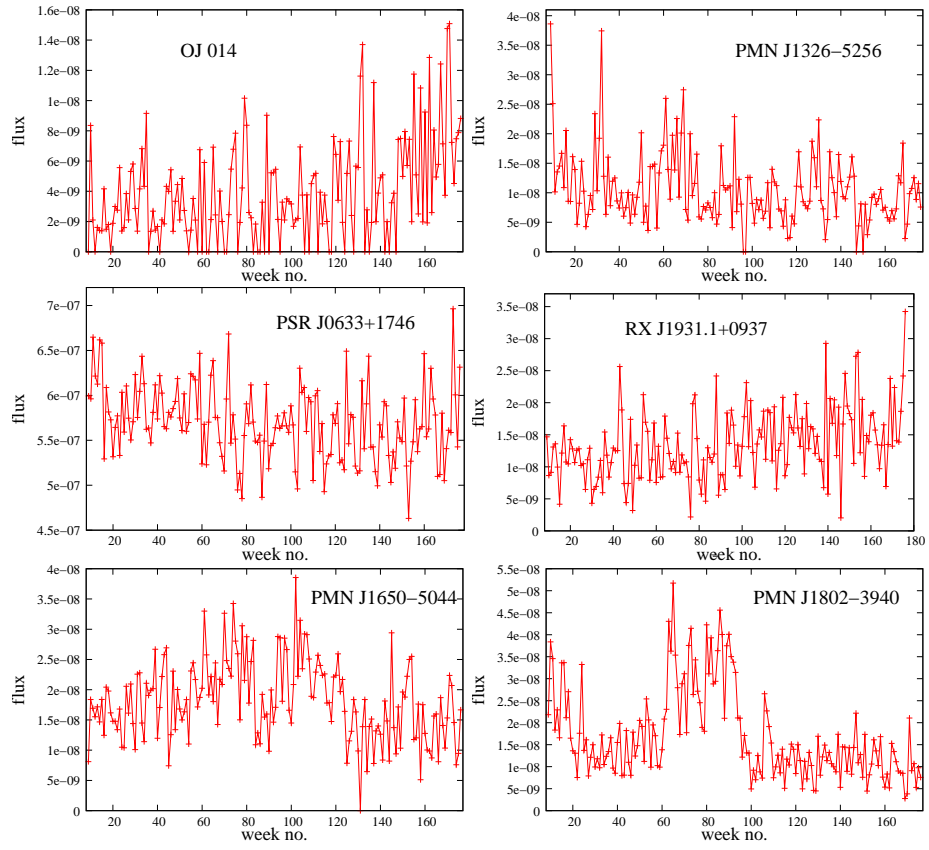


**Fig. 7.** The same as in Figure 5.

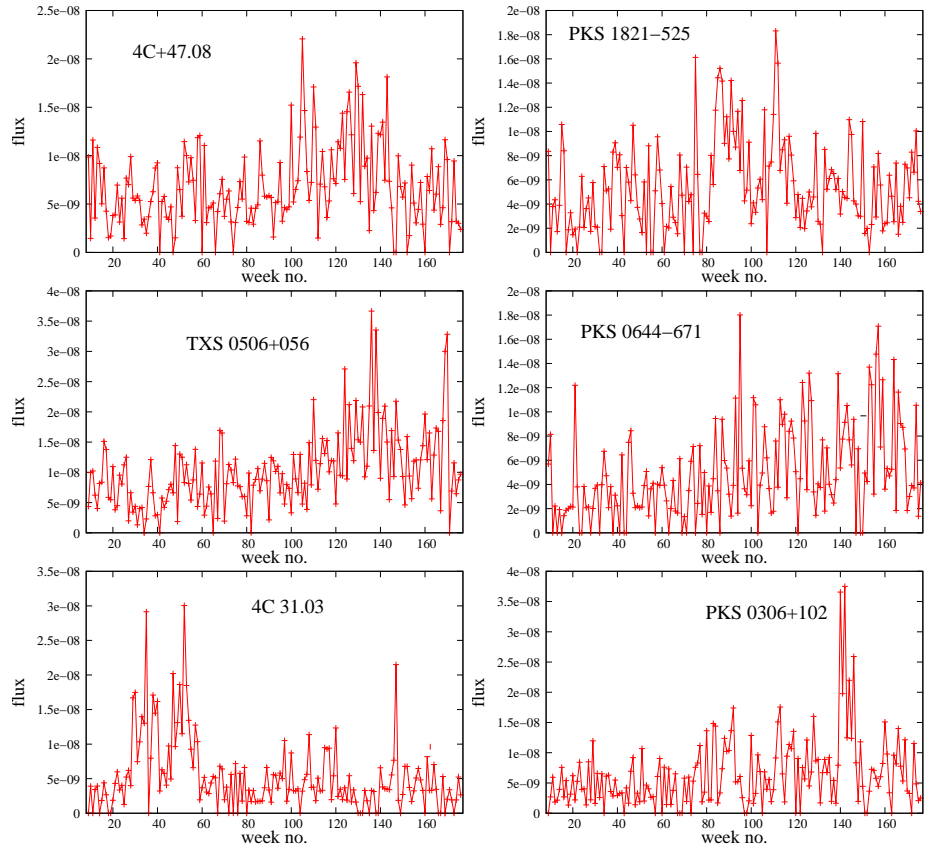


**Fig. 8.** The same as in Figure 5.

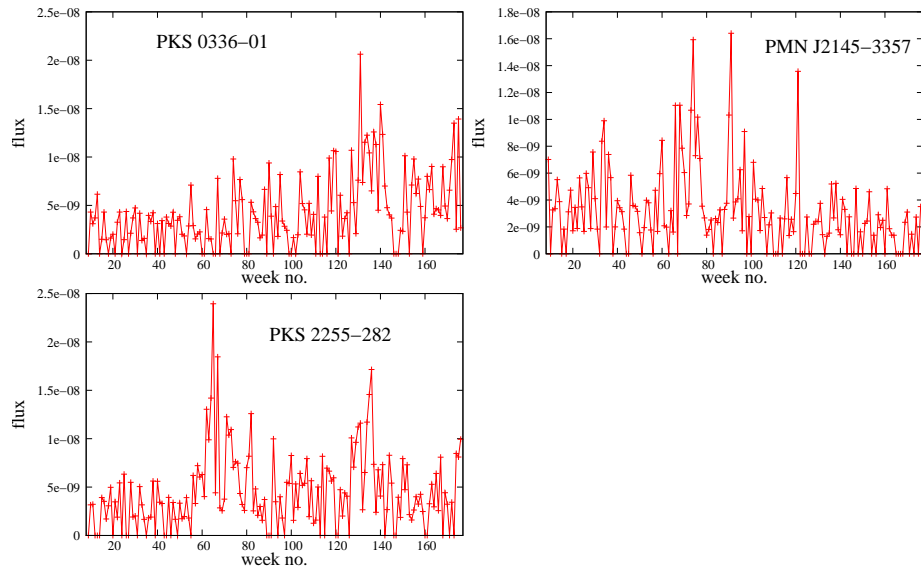


**Fig. 9.** The same as in Figure 5.